Modeling Stress Effects in Magnetic Thrust Bearings Using Finite Elements

P. T. DEPRET-GUILLAUME,[1] D. W. LEWIS[1] AND R. R. HUMPHRIS[1]

ABSTRACT

Magnetic thrust bearings in rotating machinery have been studied for several years. This paper examines the effect of modeling different stress dependent B–H curves in the thrust disk using a commercial finite element magnetic circuit solver. One thrust bearing configuration is analyzed and two solutions are compared. The results for a stress free (sf) bearing and a bearing modeling tension (t) and compression (c) are reported.

INTRODUCTION

Work in electromagnetic bearings arose from limitations and problems with traditional bearings used in turbo machinery such as gas turbines, jet engines, pumps and compressors. In recent years, magnetic bearing research has produced a wealth of information in the areas of controls, rotor dynamics, power amplifiers and actuator/bearing designs. Magnetic suspension technology has been available for years, including devices such as the 800,000 revolutions per second miniature ball support [1], canned motor pumps, aircraft compressors and turbines. Space applications include platform supports, telescopic pointing devices and flywheels.

Implementation of magnetic bearing systems have several advantages over other traditional types of bearings such as fluid film and ball bearings. Lubricants of some type are needed for fluid film bearing operation. Operating temperature limitations of the lubricants and the fire hazard of certain lubrication fluid supply systems are two problem areas that may be eliminated by the use of magnetic bearings. Further, weight savings from elimination of lubricant supply systems may be an advantage in some applications. Magnetic bearings are non–contacting and therefore do not need a lubricant system. Magnetic bearings eliminate the wear typically found in rolling element and fluid film bearings. Magnetic bearings also have the advantage of controllable variable stiffness and damping parameters, which provide the opportunity for better control of the vibrations and dynamic unbalance encountered in rotating machinery.

[1] University of Virginia, Department of Mechanical and Aerospace Engineering, McCormick Rd., Charlottesville, Virginia, 22903

The disadvantages of magnetic bearing systems are the high cost of development, relatively low ratio for load capacity to bearing actuator weight ratio and an inability to carry loads exceeding the bearing design load capacity for any great length of time. The per unit cost should significantly decrease once magnetic bearing systems are mass produced for implementation into given pump/jet engine/turbine products and not just developed on a project/prototype/retrofit basis. The low load capacity to bearing actuator weight ratio as compared to traditional bearings can be increased by using higher saturation density magnetic material such as cobalt iron and related alloys. Again, cobalt irons are more expensive than silicon iron, but as the demand for these materials increase, the cost should decrease. Lastly, temporary loads exceeding the nominal design load capacity may be handled by designing the system to operate in the saturated region of the B–H curve.

In the past and present, bearing designs have been confined to a linear region of the flux carrying capacity of the material. This yields bearings that are over designed to ensure that the heating losses are minimized and the maximum flux density remains below the saturation point on the B–H curves for the material. The advent of faster personal computers has allowed the designer to use main frame type finite element programs [2, 3] to solve problems originally solved analytically [4].

The core materials used in magnetic bearings include pure iron, cobalt iron, and nickel ferrites, with variations of each depending on what properties the designer needs for a given application. Bozorth [5] summarizes the properties of a wide range of materials. Moses and Thomas [6] have done extensive work with cobalt iron and its alloys. Their work includes magnetic characteristics under high stress conditions. Fiedler, Habermehl et al, Moses and Thomas [7, 8, 9, 10] have reported on heat treatments of iron cobalt. Research by Besnus and Meyer, Jacobs and Major et al [11, 12, 13] has been done in the area of element additions into iron cobalt in order to improve or optimize the magnetic/mechanical properties of the iron cobalt material.

NOMENCLATURE (See Figure 2)

A_1	Area of inner pole	d_7	Outer diameter of stator
A_2	Area of middle pole	F_1	Force on inner pole
A_3	Area of outer pole	F_2	Force on middle pole
B	Magnetic flux density	F_3	Force on outer pole
d_1	Inner diameter of stator	F_{in}	Force of inner magnet
d_2	Inner diameter of inner coil	F_{out}	Force of outer magnet
d_3	Outer diameter of inner coil	F_{rat}	Force ratio (F_{out}/F_{in})
d_4	Diameter for design purposes	F_{tot}	Total Force
d_5	Inner diameter of outer coil	Ni	Magnetizing field
d_6	Outer diameter of outer coil		

BACKGROUND AND PROCEDURE

STRESS DEPENDENCE OF IRON COBALT MATERIALS

The magnetic properties of most materials are dependent on the magnetizing force field H and the temperature. Stresses applied to the material also change the magnetic properties. Each material is affected differently by different stress

conditions. Material under tension can have large increases in permeability for a given H while other materials decrease in permeability when subject to tension. Positive and negative magnetostriction terms are defined by Bozorth [5]. Positive magnetostriction is present when the magnetization is increased by tension whereas negative magnetostriction is defined by a decrease in magnetization in the presence of tension. Positive magnetostriction is also characterized by the expansion of the material. The opposite is true for negative magnetostriction. The expansion or contraction of the material is due to the magnetic forces and the elastic forces between atoms coming to equilibrium. The finite element analysis does not directly account for the magnetostrictive effects.

In 1975, Moses and Thomas [6] studied the effects of stress on the DC magnetization properties of Permendur 49Co–49Fe–2V. The work included data collected on two samples of laminations obtained from vendors. They concluded that tension always has a beneficial effect on the B–H characteristics and compression has the opposite effect. In high speed machine rotors, they recommend permendur annealed at 650°C (1202°F) for one hour as having the best mechanical properties under tension. The industrial standard is to anneal at 760°C (1400°F). Figure 1 shows induction versus magnetizing field curves under the three possible load conditions, stress free (sf), tension (t) and compression (c), for materials annealed at 760°C (1400°F). The levels of stress are ±300 Mpa (±43,500 psi). Moses and Thomas conclude that compression always has a detrimental effect on the B–H curve.

RESULTS

The information on the stress dependent iron cobalt material can be used in the finite element software in order to determine the stress effects on the thrust bearing design load capacity. First, a sketch of the bearing geometry is given in Figure 2, which shows a general EI type of bearing design. The "E" represents the stator cross section, while the "I" stands for the rotor thrust disk or collar cross section. The design can be more easily visualized by considering the magnet as two conventional single acting thrust bearings with one bearing's (called the inner bearing) outer radius or diameter marking the inner diameter of the second bearing (called the outer bearing), this point occurring somewhere between d_3 and d_5. The bearing's length, load capacity, and inner diameter fix the bearing's outer diameter and cross sectional profile. The load capacities of the inner and outer bearings have to be iterated upon until the cross sectional profiles are the same. F_{in} and F_{out} define the load capacities of the inner and outer bearings, respectively. The ratio of F_{out} to F_{in} is called F_{rat}. Together, the inner (A_1) and outer (A_3) areas of the EI bearing produce one half of the total load capacity of the bearing, while the middle area (A_2) produces the other half. Now there exists a procedure where by the designer needs to go through four iterations to get matching cross sections.

Next, the force between the stator and thrust disk can be determined. First, the material regions are identified such that the output file gives the average flux density, B, in the air gaps. Once the pole face areas, A_1, A_2 and A_3, are defined and the flux density B is determined, the load capacity can be easily calculated.

The completed model for the stress free (sf) bearing can be changed to a model for tension (t) and compression (c) by simply editing the ascii input file.

The output file (See Appendix A) can be very informative if the geometry is chosen correctly. This file summarizes the material information and gives the maximum, average, and minimum flux density for each material identity defined in

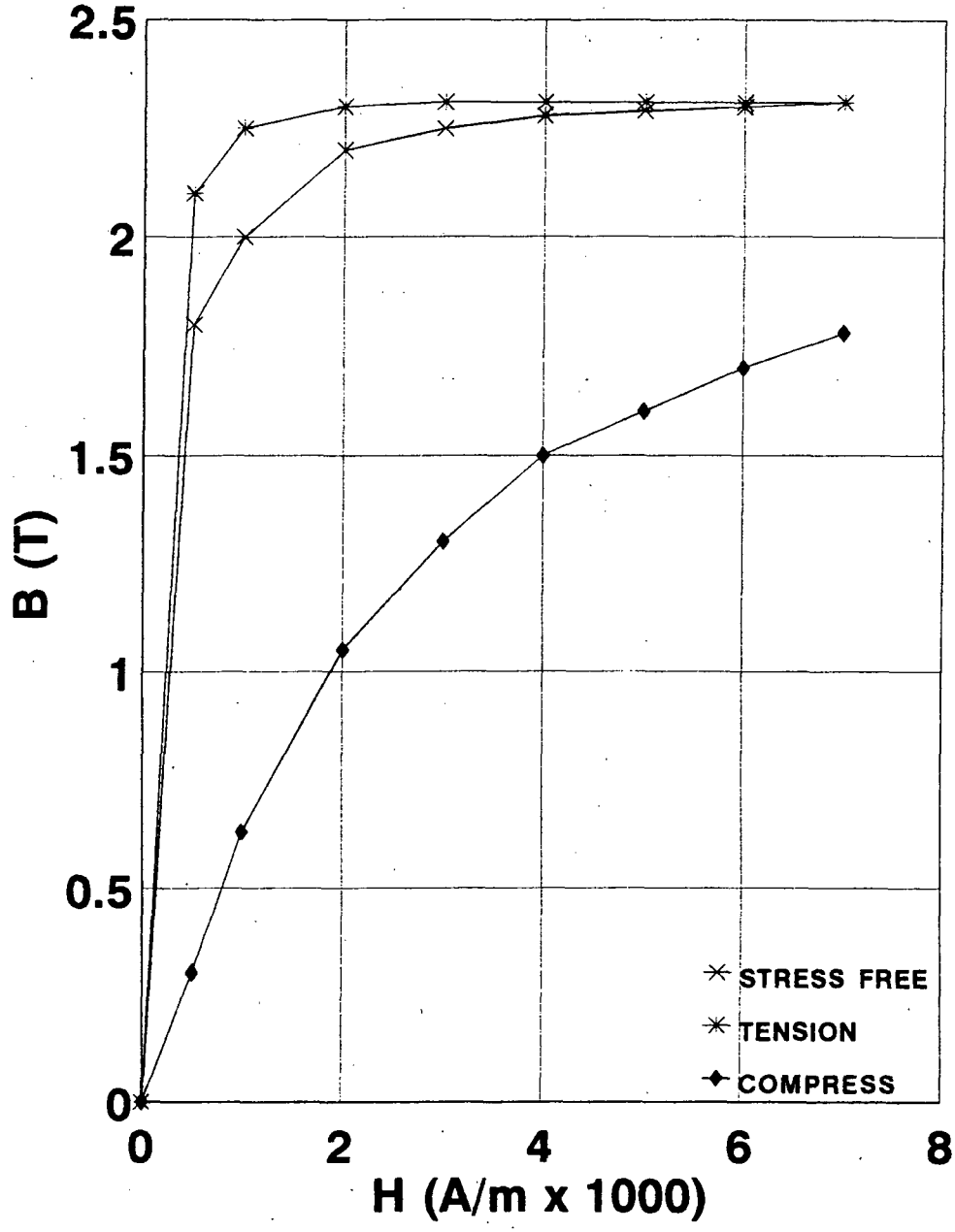

FIGURE 1. B–H CURVES [6] FOR THREE STRESS CONDITIONS: STRESS FREE (sf), TENSION (t) AND COMPRESSION (c) FOR PERMENDUR (49% COBALT, 49% IRON, 2% VANADIUM) (±300 MPa or ±43,500 psi)

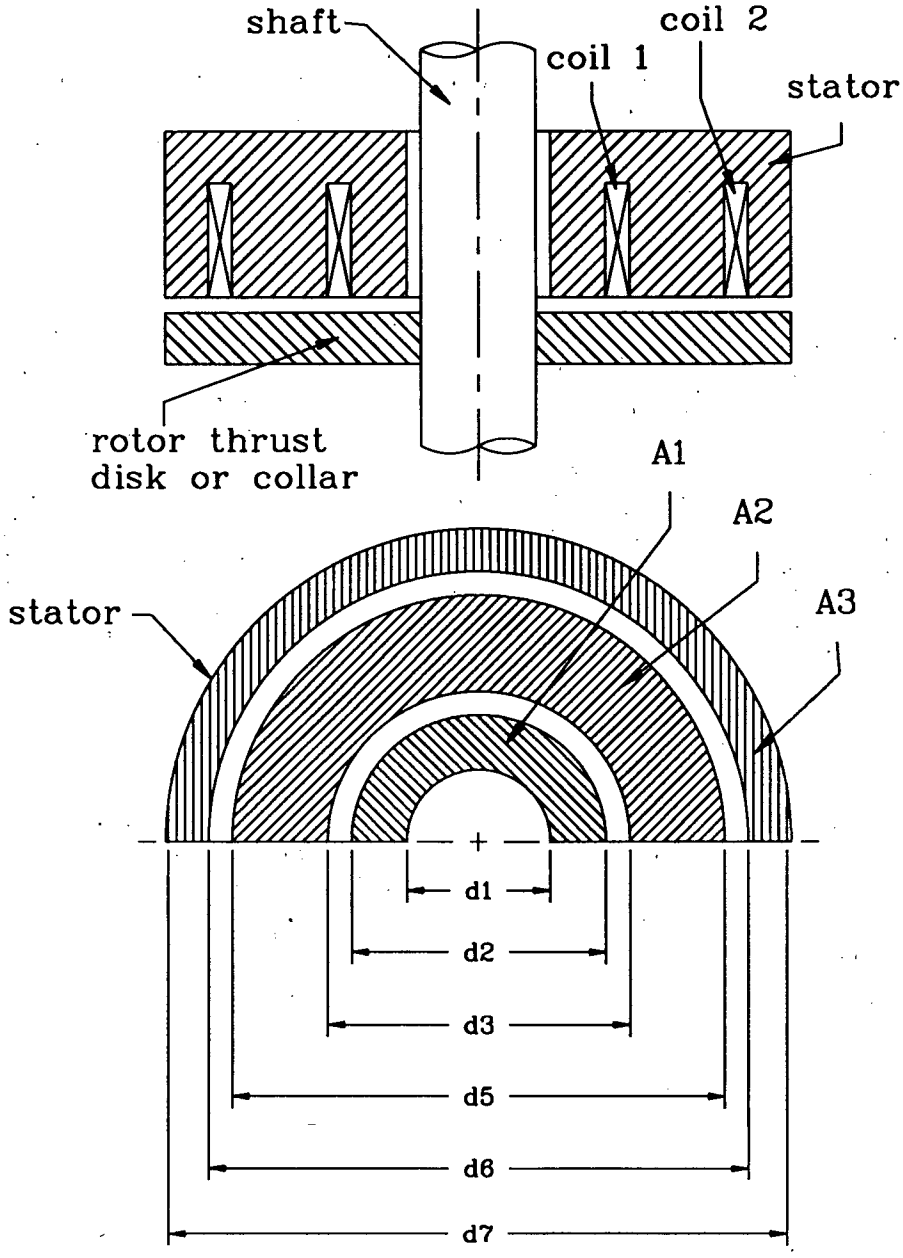

FIGURE 2. GENERAL EI TYPE THRUST BEARING DESIGN

the finite element model. For example, if the geometry for the thrust base is divided under two region IDs, 7 and 14, as shown in Figure 3, then, in the output file under the summary for materials 7 and 14, the three flux densities will be given. The region IDs are defined for the two models. The region IDs for the different stresses are shown in Table I. Depending on which model is used, the stress in region ID 5 can be either in a compressive (c) or stress free state (sf). Similarly, the stress in region ID 12 can be either in a tension (t) or stress free (sf) state. Table II summarizes the average flux density in Teslas for the bearings in the stress free (sf) and tension/compression condition.

The results for modeling the tension and compression in the thrust disk produced a significant reduction in bearing load capacity for the non–rotating case. The model for the rotating case was not evaluated, because the model would yield a bearing with a larger load capacity than the unstressed model.

Tables III and IV summarize the force for all three pole face areas. The reduction in F_{tot} is about 11.2% due to the compression in the one–third of the thrust disk closest to the air gap, identified as material region number 5 in Table I. See Figure 3 for locating the material region numbers. An almost identical result is noted if the load capacity is calculated using the information recorded for the air gaps, regions 2 and 9, where the both flux densities decrease by 5.7%. This method indicates an 11.1% reduction in load capacity. As can be calculated from Table II, the flux density in material 5 decreases by 17.6% whereas the other two portions of the thrust collar or disk are compensating, evidenced by an increase in flux density. The stress free section, region 8, and the tension section, region 12, have increased by 24.7 and 38.8% in the flux density values, respectively.

CONCLUSION

The stress effects on the load capacity of the magnetic thrust bearing indicate an overall reduction of 11.2%. In the case of stress in the thrust disk, the tension and stress free sections are noted to compensate for the decrease in flux density in the compression section, but when examined as a whole, the detrimental effects of the reduced flux densities, with the corresponding lower load capacities, remain.

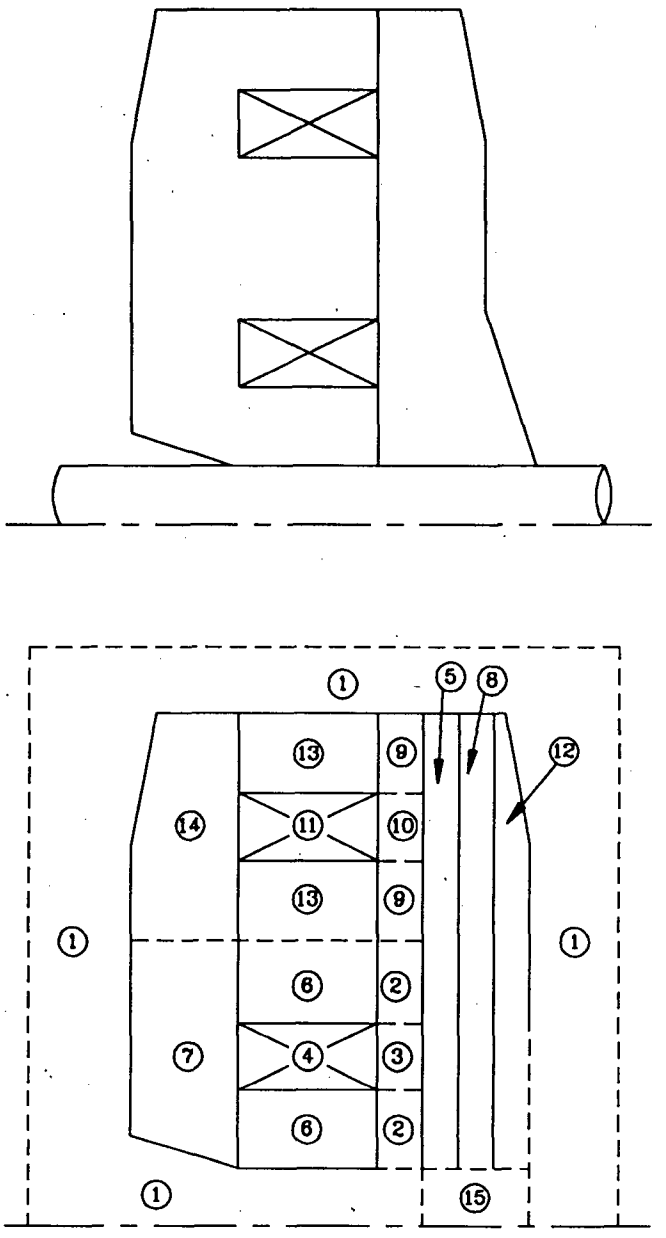

FIGURE 3. REGION ID USED IN MSC/MAGGIE FEM MODEL FOR PERMENDUR IN STRESS FREE AND TENSION/COMPRESSION CONDITIONS (AIR GAP NOT TO SCALE) (SHAFT AND TAPER NOT MODELED)

TABLE I
PARTITIONING OF GEOMETRIC REGION IN FEM MODEL FOR STRESS EFFECTS

Region ID	Material	Description of Location
1	air	region enclosing whole bearing
2	"	inner magnet air gaps
3	"	inner magnet air gap bet. coil and thrust collar
4	"	inner magnet coil cross section
5	Permendur	inner 1/3 of thrust collar closest to air gap in compression (c) or stress free (sf)
6	"	inner magnet material above and below the inner coil
7	"	inner magnet of thrust base
8	"	middle 1/3 of thrust collar stress free (sf)
9	air	outer magnet air gap
10	"	outer magnet air gap bet. coil and thrust collar
11	"	outer magnet coil cross section
12	Permendur	outer 1/3 of thrust collar in tension (t) or stress free (sf)
13	"	outer magnet material above and below the outer coil
14	"	outer magnet of thrust base
15	"	thrust collar portion not specifically used for magnetic path

TABLE II
SUMMARY OF AVERAGE FLUX DENSITY FOR STRESS FREE AND TENSION/COMPRESSION

Material Region ID #	B average (T)	
	Stress Free	Tension and Compression
1	0.00434	0.00427
2	1.412	1.331
3	0.0430	0.0451
4	0.0582	0.0586
5	1.499	1.235
6	1.441	1.360
7	1.081	1.003
8	1.054	1.314
9	1.420	1.339
10	0.0439	0.0461
11	0.0587	0.0591
12	0.742	1.030
13	1.467	1.386
14	1.222	1.138
15	0.0141	0.0141

TABLE III
FORCES CALCULATED FOR STRESS FREE (SF)
CONDITION FOR EI BEARING MADE OF 2V PERMENDUR.

OUTER MAGNET

A_3

Element*	F(N)
1	2746
2	2646
3	2563
4	2481
	10436 = 2346.0 lb

A_2

Element*	F(N)
1	1988
2	1917
3	1825
4	1732
5	1643
6	1556
	10661 = 2396.6 lb
	4742.6 lb = F_{out}

INNER MAGNET

A_2

Element*	F(N)
7	1535
8	1451
9	1370
10	1290
	5646.0 = 1269.2 lb

A_1

Element*	F(N)
1	1242
2	1116
3	982.8
4	850.5
5	720.9
6	591.8
	5503.5 = 1237.2 lb
	2506.4 lb = F_{in}

$F_{in} + F_{out} = F_{tot} = 7249.0$ lb

TABLE IV
FORCES CALCULATED FOR TENSION (T) AND COMPRESSION (C)
STRESS CONDITIONS FOR EI BEARING MADE OF 2V PERMENDUR.

OUTER MAGNET

A_3

Element*	F(N)
1	2398
2	2311
3	2274
4	2271
	9254 = 2080.3 lb

A_2

Element*	F(N)
1	1794
2	1732
3	1619
4	1523
5	1438
6	1358
	9464 = 2127.5 lb
	4207.8 lb = F_{out}

INNER MAGNET

A_2

Element*	F(N)
7	1337
8	1275
9	1218
10	1181
	5011.0 = 1126.5 lb

A_1

Element*	F(N)
1	1128
2	1004
3	869.0
4	745.4
5	628.6
6	516.1
	4891.1 = 1099.5 lb
	2226.0 lb = F_{in}

$F_{in} + F_{out} = F_{tot} = 6433.8$ lb

REFERENCES

1. Beams J. W. et al, U. S. Patent No. 2,691,306, Oct 12, 1954.

2. MSC/MAGGIE supplied by MacNeal–Schwendler Corporation.

3. PC\Magnetic supplied by ANSYS.

4. Banerjee B. B., Analysis and Design of Magnetic Thrust Bearings, Thesis University of Va., June 1988.

5. Bozorth R. M., Ferromagnetism, New York: D Van Nostrand, p190–209, 1951.

6. Moses A. J. and Thomas B., "Effects of stress on D.C. magnetization properties of Permendur", Proceedings Institution of Electrical Engineers, Vol. 122, No. 7, p761–762, Jul. 1975.

7. Fiedler H. C., "Optimizing the combination of magnetic induction and yield strength of vanadium Permendur by heat treatment", AIP Conf. Proc., No. 24, p739–740, 1974.

8. Habermehl S., Jiles D. C. and Teller C. M., "Influence of Heat Treatment and Chemical Composition on the Magnetic Properties of Ferromagnetic Steels", IEEE Transactions on Magnetics, Vol. 11, No. 5, Sep. 75.

9. Moses A. J., "The influence of heat treatment on magnetic properties of a soft iron cobalt alloy", in AIP Conf. Proc., No. 24, p741–742, 1974. Need to look for or make a search.

10. Thomas B., "The optimum heat treatment for cobalt–iron–vanadium alloy for use in high speed airborne generators", in EPS Conf. Proc. on Soft Magnetic Materials, p109–114, Apr. 1975.

11. Besnus M. J. and Meyer A. J. P., "Magnetization Measurements of 0, 5, 10, 20 at. % Al–Substituted first–transition–series alloys", Physical Review B, Vol. 2 No. 8, p2999–3004, Oct. 1970.

12. Jacobs I. S.,"Magnetic Properties in the System Iron–Cobalt–Aluminum", IEEE Transactions on Magnetics, Vol. 21 No. 4, Jul 85.

13. Major R. V.,Martin M. C. and Branson M. W., "The development of Co–Fe soft magnetic alloy with improved mechanical properties for use in aircraft electrical generators", Inst.Elec. Eng. Conf. Proc.,Advances in Magnetics, Sep. 1976.

APPENDIX A : FINITE ELEMENT SOFTWARE

The information presented in this paper can be used in a finite element software [2]. The program is menu driven but it has the flexibility to convert the FEA file (filename.FEM) used by the program to an ascii file (filename.DAT or the input file) that the user can change easily for small variations in the model (i.e. different B–H curves or different coil currents). Filename.F06 is the output file.

The model building process is divided into three stages called Pre–processor, Processor, and Post–processor. The Pre–processor deals with building the model. This includes five steps; geometry (GEOM), region (REGION), mesh (MESH), material (MAT) and solution (SOLU). The program allows the user to input a geometry (i.e. thrust bearing) that defines a magnetic circuit using the commands found under the GEOM menu. Using the commands located in the REGION menu, the user then must assign materials (air gap and iron alloys) to given regions defined by the geometry input. Next, the loads (i.e. the coil current times the number of conductors that drives the magnetic circuit) must be assigned to some air region previously defined. Lastly, the boundary conditions, called SPEC, must be included in the model. The boundary conditions and load commands are found under the REGION menu also. The MESH menu allows the user to divide the geometry input into smaller pieces before the mesh is generated. The MAT menu allows the material properties to be defined. Non–linear materials can be modeled if the B–H curve for the material is known. The last menu, SOLU, allows the user to define the parameter of the solution. These include setting the number of iterations, type of analysis, units, loads and constraints to include frequencies in case of AC analysis and two dimension or axisymmetric geometry.

The Processor is that portion of the program which solves the circuit model input. This step in the analysis consists of waiting for a solution. The program will create files, one of which stores the solution in tabulated form, called filename.F06 file. Another file is read by the program for viewing the solution on the monitor in the Post–processor stage.

This magnetic thrust bearing model is axisymmetric about the y–axis. A condition of zero flux has been set at the modeled air boundaries around the thrust bearing.